JOURNAL OF AIRCRAFT
Vol. 44, No. 5, September–October 2007

Thermal Buckling and Nonlinear Flutter Behavior of Functionally Graded Material Panels

Hesham Hamed Ibrahim*
Noon for Research and Development, Cairo, Egypt
Mohammad Tawfik†
German University in Cairo, Cairo, Egypt
and
Mohammed Al-Ajmi‡
Kuwait University, 13060 Safat, Kuwait

DOI: 10.2514/1.27866

The nonlinear flutter and thermal buckling of an functionally gradient material panel under the combined effect of elevated temperature conditions and aerodynamic loading is studied. A nonlinear finite element model based on the first-order shear deformable plate theory and von Kármán strain-displacement relations is adopted. The governing nonlinear equations are obtained using the principal of virtual work, adopting an approach based on the thermal strain being a cumulative physical quantity to account for temperature-dependent material properties. The aerodynamic pressure is modeled using the quasi-steady first-order piston theory. This system of nonlinear equations is solved by the Newton–Raphson numerical technique. It is found that the temperature increase has an adverse effect on the functionally gradient material panel flutter characteristics through decreasing the critical dynamic pressure. Decreasing the volume fraction enhances flutter characteristics, but this is limited by structural integrity aspect. The presence of aerodynamic flow results in postponing the buckling temperature and in suppressing the postbuckling deflection, and the temperature increase gives way for higher limit-cycle amplitude.

Introduction

THE external skin of high-speed flight vehicles experiences high temperature rise due to aerodynamic heating, which can induce thermal buckling and dynamic instability. In general, thermal buckling does not indicate structural failure. However, the thermal large deflections of the skin panels can change its aerodynamic shape, causing reduction in the flight performance.

A comprehensive literature review on thermally induced flexure, buckling, and vibration of plates and shells was presented by Tauchart [1] and Thornton [2]. Gray and Mei [3] investigated the thermal postbuckling behavior and free vibrations of thermally buckled composite plates using the finite element method. Shi and Mei [4] solved the problem of thermal postbuckling of composite plates with initial imperfections using the finite element modal method. The modal participation values of linear postbuckling modes was defined and used to determine the minimum number of modes needed for convergence. The equations of motion were derived using the principal of virtual work. The temperature change over the plate is considered to be a large steady-state temperature change over the plate $\Delta T(x, y)$. Jones and Mazumdar [5] investigated the linear and nonlinear dynamic behavior of plates at elevated temperatures. They presented analytical solutions for the thermal buckling and postbuckling behavior of a plate strip. A general formula is also presented that links the fundamental frequency of vibration to the critical buckling temperature and the corresponding frequency of the unheated plate. Shi et al. [6] investigated the thermal postbuckling behavior of symmetrically laminated and antisymmetric angle-ply laminated composite plates and the deflection of asymmetrically laminated composite plates under mechanical and thermal loads. A finite element formulation in modal coordinates was developed for the nonlinear thermal postbuckling of thin composite plates. The quantitative contribution of each linear buckling mode shape to the postbuckling deflection was shown.

Panel flutter is a phenomenon that is usually accompanied by temperature elevation on the outer skin of high-speed air vehicles. Panel flutter is a self-excited oscillation of a plate or shell in supersonic flow. Because of aerodynamic pressure forces on the panel, two eigenmodes of the structure merge and lead to this dynamic instability. Supersonic flutter of plates and shells was recognized to be an important aspect of the design of high-speed vehicles when Jordan [7] observed that a number of the early V-2 rocket failures were due to panel flutter. Since then, extensive analytical and experimental research on that subject has been performed. A common remedy to the flutter problem is to stiffen those panels in danger of flutter, a method that usually introduces additional weight to the design. Thin plates are a commonly used form of structural components, especially in aerospace vehicles such as high-speed aircraft, rockets, and spacecrafts, which are subjected to thermal loads due to aerodynamic and/or solar radiation heating. This results in a temperature distribution over the surface and thermal gradient through the thickness of the plate. The presence of these thermal fields results in a flutter motion at lower dynamic pressure or a larger limit-cycle amplitude at the same dynamic pressure. Accordingly, it is important to consider the interactive effect of both aforementioned failure characteristics (flutter and thermal buckling).

A vast amount of literature exists on panel flutter using different aerodynamic theories to model the aerodynamic pressure and different structure models [8–16].

Extensive research work has been carried out on the FGM since its concept was proposed in the late 1980s in Japan. FGMs are nonhomogeneous composites characterized by a smooth and

Received 17 September 2006; revision received 10 April 2007; accepted for publication 5 June 2007.

*Researcher, Vibration and Acoustics Control Center; Hesham.ibrahim@noonrd.org.

†Assistant Professor, Modeling and Simulation in Mechanics Department; Mohammad.Tawfik@guc.edu.eg.

‡Assistant Professor, Mechanical Engineering Department, College of Engineering and Petroleum, P.O. Box 5969; malajmi@kuc01.kuniv.edu.kw.

continuous change of material properties from one surface to the other. This is achieved by gradually varying the volume fraction of the constituent materials. One of the advantages of using these materials is that they can survive environments with high temperature gradients while maintaining structural integrity. Functionally graded materials are usually composed of two or more materials for which the volume fractions are changing smoothly and continuously along the desired direction(s). This continuous change in the compositions leads to a smooth change in the mechanical properties, which has many advantages over the laminated composites, for which the delamination and cracks are most likely to initiate at the interfaces, due to the abrupt variation in the mechanical properties between laminas [17].

Dai et al. [17] presented a mesh-free model for the active shape control and the dynamic response suppression of a functionally graded material plate containing piezoelectric sensors and actuators. Birman [18] studied the stability of functionally graded shape memory alloy hybrid sandwich panels under the simultaneous action of in-plane compressive and thermal loadings. Functional grading was achieved by a nonuniform distribution of shape memory alloy fibers in the middle plane (sinusoidal distribution). El-Abbasi and Meguid [19] presented a new thick-shallow-shell element to study the thermoelastic behavior of functionally graded structures made from shells and plates. The element accounts for the varying elastic and thermal properties across its thickness. Reddy [20] presented theoretical formulation, Navier's solutions of rectangular plates, and a finite element model based on the third-order shear deformation plate theory for the analysis of through-the-thickness functionally graded plates. The formulation accounts for the thermomechanical coupling, time dependency, and von-Kármán-type geometric nonlinearity.

He et al. [21] presented a finite element formulation based on the classical laminated plate theory for the shape and vibration control of functionally graded material plates with integrated piezoelectric sensors and actuators. A constant velocity feedback control algorithm was used for the active control of the dynamic response of the FGM plate through closed-loop control. Javaheri and Eslami [22] derived the equilibrium and stability equations of a rectangular plate made of a functionally graded material under thermal loads, adopting the higher-order shear deformation plate theory. A buckling analysis of a functionally graded plate under four types of thermal loads was carried out, and a closed-form solution for the prediction of the buckling temperature for rectangular simply supported FGM plates was obtained. Woo et al. [23] developed an analytical solution for the postbuckling behavior of plates and shallow cylindrical shells made of functionally graded materials under the simultaneous action of compressive in-plane loads and a temperature field. The solution is obtained in terms of a mixed Fourier series.

Yang et al. [24] investigated the geometrically nonlinear bending behavior of functionally graded plates with integrated piezoelectric layers and subjected to transverse loads and a temperature gradient through the plate thickness. Reddy's [20] higher-order shear deformation plate theory was adopted. Zenkour [25] studied the static response for a simply supported functionally graded rectangular plate subjected to a transverse uniform load using a generalized shear deformation theory. The effects of transverse shear deformation, plate aspect ratio, side-to-thickness ratio, and volume fraction distributions were presented. It was found from the analysis that the response of an FGM plate is intermediate to that of the ceramic and metal homogeneous plates.

Kim [26] developed an analytical technique to investigate the effect of temperature on the vibration characteristics of thick functionally graded rectangular plates, taking into account the temperature dependence of the material properties. Batra and Jin [27] adopted the first-order shear deformation theory (FSDT) coupled with finite element method to study the vibration of functionally graded anisotropic rectangular plates with different edge-support conditions. The grading there was achieved through continuously changing the fiber orientation angle through the thickness. Qian and Batra [28] adopted the meshless local Petrov– Galerkin method and the compatible higher-order shear and normal deformation plate theory to a thick, two-constituent, functionally graded cantilever plate. The volume fractions of the constituents were assumed to vary in the x and y directions. The spatial volume fractions of the constituents are optimized to maximize either the first or the second natural frequency of the plate. Parkash and Ganapathi [29] adopted the finite element method to investigate the supersonic flutter behavior of flat panels made of functionally graded material under the influence of thermal environment. Temperature-dependent material properties were only assumed when calculating material properties through the thickness, but not when increasing the temperature to reach buckling. Typically, the FGMs are made of a mixture of two materials: a ceramic that is capable of withstanding high-temperature environments, due to its low thermal conductivity, and a metal that acts as a structural element to support loading and prevent fractures. Without losing generality, it is usually assumed that the top surface of an FGM plate is ceramic-rich and that the bottom surface is metal-rich. The region between the two surfaces consists of a blend of the two materials, which is assumed in the form of a simple power law distribution as [17]

$$P_e(z) = P_C V_C + P_M(1 - V_C) \tag{1}$$

$$V_C = \left(0.5 + \frac{z}{h}\right)^n, \qquad (-h/2 \le z \le h/2, 0 \le n \le \infty) \tag{2}$$

where z is coordinate in the thickness direction of a plate; P_e, P_C, and P_M are effective material properties of the FGM, the properties of the ceramic, and the properties of the metal, respectively; V_c is the ceramic volume fraction; h is the plate thickness; and power n is the volume fraction exponent. Figure 1 shows the variation of the volume fraction function versus nondimensional thickness with different volume fraction exponents n. Functional grading could be also achieved through smoothly changing the fiber orientation of a composite laminate through the plate thickness or through a nonuniform distribution of the fibers in the plane of the plate [18]. In this work, the nonlinear flutter and thermal postbuckling behavior of a ceramic-metal functionally graded plate under thermal and aerodynamic loadings is studied using nonlinear finite element method. The nonlinear governing equations for a thick, rectangular, functionally graded plate are obtained using the principle of virtual work and the von Kármán strain-displacement relation. The approach is based on thermal strain being a cumulative physical quantity, whereas the stress is an instant quantity. Thus, the thermal strain is an integral quantity of thermal expansion coefficient with respect to temperature, whereas stress is evaluated with the instant elastic modulus at certain temperatures in the thermoelastic stress–strain relations [30]. Therefore, the method does not need the many small increments as in the incremental method [31], and it is suitable for any nonlinear temperature-dependent material properties. Numerical results are provided to show the effects of thermal field,

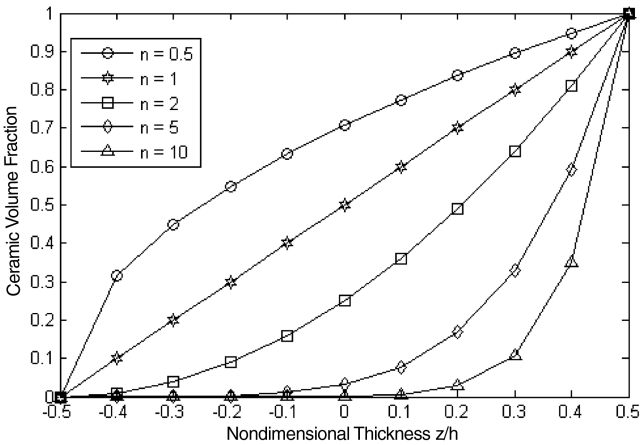

Fig. 1 Variation of the ceramic volume fraction function versus the nondimensional thickness z/h.

material properties, volume fraction exponent, and boundary conditions on the postbuckling, fundamental frequency, critical dynamic pressure, and limit-cycle amplitude of a functionally graded rectangular plate. To the authors' knowledge, this is the first time that the shear deformable plate theory has been applied with the cumulative thermal strain concept in the thermal buckling and nonlinear flutter of FGM plates.

Finite Element Formulation of Thermal Postbuckling of FGM Panels

The equations of motion with the consideration of moderately large deflection and temperature-dependent material properties are derived for a functionally graded plate subject to aerodynamic and thermal loadings. To account for temperature dependence of material properties, a cumulative thermal strain is adopted for the calculation of the thermal deflection and stresses in the plate. The element used in this study is the rectangular, nine-node, C^0, nonconforming element (for the bending DOF).

Displacement/Nodal-Displacement Relation

The degree-of-freedom vector of the rectangular plate element can be written

$$\{\delta\} = \{[w], [\phi_x, \phi_y], [u, v]\} = \begin{Bmatrix} \{w_b\} \\ \{w_\phi\} \\ \{w_m\} \end{Bmatrix} \tag{3}$$

where w is the transverse displacement; ϕ_x and ϕ_y are the rotations of the transverse normal about the x and y axes, respectively; u and v are the membrane displacements in the x and y directions, respectively; $\{w_b\}$ is the nodal transverse displacement vector; $\{w_f\}$ is the nodal rotation of the transverse normal vector; and $\{w_m\}$ is the nodal membrane displacements vector.

The displacement/nodal-displacement relation can be presented in terms of interpolation function matrices $[N_w]$, $[N_{\phi x}]$, $[N_{\phi y}]$, $[N_u]$, and $[N_v]$ as

$$\begin{gathered} w = [N_w]\{w_b\}, \qquad \phi_{\mathrm{x}} = [N_{\phi_x}]\{\mathrm{w}_\phi\}, \qquad \phi_{\mathrm{y}} = [N_{\phi_y}]\{\mathrm{W}_\phi\} \\ u = [N_u]\{W_m\}, \qquad v = [N_v]\{W_m\} \end{gathered} \tag{4}$$

Nonlinear Strain-Displacement Relation

The in-plane strains and curvatures, based on the von Kármán moderately large deflection and first-order shear deformable plate theory, are given by

$$\begin{Bmatrix} \varepsilon_x \\ \varepsilon_y \\ \gamma_{xy} \end{Bmatrix} = \begin{Bmatrix} \frac{\partial u}{\partial x} \\ \frac{\partial v}{\partial y} \\ \frac{\partial u}{\partial y} + \frac{\partial v}{\partial x} \end{Bmatrix} + \begin{Bmatrix} \frac{1}{2}\left(\frac{\partial w}{\partial x}\right)^2 \\ \frac{1}{2}\left(\frac{\partial w}{\partial y}\right)^2 \\ \frac{\partial w}{\partial x}\frac{\partial w}{\partial y} \end{Bmatrix} + z \begin{Bmatrix} \frac{\partial \phi_y}{\partial x} \\ \frac{\partial \phi_x}{\partial y} \\ \frac{\partial \phi_y}{\partial y} + \frac{\partial \phi_x}{\partial x} \end{Bmatrix} \tag{5}$$

or, in compact form,

$$\{\varepsilon\} = \{\varepsilon_{\mathrm{lin}}\} + \{\varepsilon_\theta\} + z\{\kappa\} \tag{6}$$

where parameters u, v, and w are displacements in the x, y, and z directions, respectively; and $\{\varepsilon_{\mathrm{lin}}\}$, $\{\varepsilon_\theta\}$, and $z\{\kappa\}$ are the membrane linear strain vector, the membrane nonlinear strain vector, and the bending strain vector, respectively.

The transverse shear strain vector can be expressed as

$$\begin{Bmatrix} \gamma_{yz} \\ \gamma_{xz} \end{Bmatrix} = \begin{Bmatrix} \phi_x \\ \phi_y \end{Bmatrix} + \begin{Bmatrix} \frac{\partial w}{\partial y} \\ \frac{\partial w}{\partial x} \end{Bmatrix} \tag{7}$$

Stress–Strain Relationship of an FGM Panel

The stress–strain relations for the FSDT can be expressed as follows [32]:

$$\{\sigma\} = \begin{Bmatrix} \sigma_x \\ \sigma_y \\ \tau_{xy} \end{Bmatrix} = [Q(z,T,n)]\{\varepsilon\} - [Q(z,T,n)] \int_{T\mathrm{ref}}^{T} \{\alpha(z,\tau,n)\}\, \mathrm{d}\tau \tag{8}$$

$$\{\tau\} = \begin{Bmatrix} \tau_{yz} \\ \tau_{xz} \end{Bmatrix} = \begin{bmatrix} Q_{44}(z,T,n) & Q_{45}(z,T,n) \\ Q_{45}(z,T,n) & Q_{55}(z,T,n) \end{bmatrix} \begin{Bmatrix} \gamma_{yz} \\ \gamma_{xz} \end{Bmatrix} \tag{9}$$

where $\{\sigma\}$ and $\{\tau\}$ are the in-plane stress vector and the transverse shear vector, respectively; and $\{\alpha(z,T,n)\}$ and $[Q(z,T,n)]$ are the thermal expansion coefficient vector and the stiffness matrix of the FGM plate, respectively.

Integrating Eqs. (8) and (9) over the plate thickness, the constitutive equation can be obtained as [30]

$$\begin{Bmatrix} \{N\} \\ \{M\} \end{Bmatrix} = \begin{bmatrix} [A] & [B] \\ [B] & [D] \end{bmatrix} \begin{Bmatrix} \{\varepsilon_m\} \\ \{\kappa\} \end{Bmatrix} - \begin{Bmatrix} \{N^T\} \\ \{M^T\} \end{Bmatrix} \tag{10}$$

$$\{R\} = \begin{Bmatrix} R_{yz} \\ R_{xz} \end{Bmatrix} = \begin{bmatrix} A_{44} & A_{45} \\ A_{45} & A_{55} \end{bmatrix} \begin{Bmatrix} \gamma_{yz} \\ \gamma_{xz} \end{Bmatrix} = [A]^s\{\gamma\} \tag{11}$$

where

$$\{\varepsilon_m\} = \{\varepsilon_{\mathrm{lin}}\} + \{\varepsilon_\theta\}$$

$$([A], [B], [D]) = \int_{-h/2}^{h/2} (1, Z, Z^2)[Q(Z,T,n)]\, \mathrm{d}Z$$

$$[A^s] = \int_{-h/2}^{h/2} [Q^s(Z,T,n)]\, \mathrm{d}Z$$

$$[Q(z,T,n)] = \begin{bmatrix} \frac{E(z,T,n)}{1-\nu^2(z,n)} & \frac{\nu(z,n)E(z,T,n)}{1-\nu^2(z,n)} & 0 \\ \frac{\nu(z,n)E(z,T,n)}{1-\nu^2(z,n)} & \frac{E(z,T,n)}{1-\nu^2(z,n)} & 0 \\ 0 & 0 & \frac{E(z,T,n)}{2[1+\nu(z,n)]} \end{bmatrix}$$

$$[Q^s(z,T,n)] = \begin{bmatrix} \frac{E(z,T,n)}{2[1+\nu(z,n)]} & 0 \\ 0 & \frac{E(z,T,n)}{2[1+\nu(z,n)]} \end{bmatrix}$$

$$(\{N^T\}, \{M^T\}) = \int_{-h/2}^{h/2} \left[Q(z,T,n) \left(\int_{T_{\mathrm{ref}}}^{T} \{\alpha(z,\tau,n)\}\, \mathrm{d}\tau \right) \right] (1, z)\, \mathrm{d}z$$

where $[A]$, $[A]^s$, $[B]$, and $[D]$ are the laminate stiffness matrices, respectively; $\{N\}$, $\{M\}$, and $\{R\}$ are the resultant vectors of the in-plane force, moment, and transverse shear forces; $\{N^T\}$ and $\{M^T\}$ are the in-plane thermal load and thermal bending moment, respectively; T denotes the temperature rise; and a constant temperature distribution in the x, y, and z directions is assumed.

Aerodynamic Loading

The first-order quasi-steady piston theory for supersonic flow states that [31]

$$P_a = -\left(\frac{g_a}{\omega_o} \frac{D_{11}}{a^4} \frac{\partial w}{\partial t} + \lambda \frac{D_{11}}{a^3} \frac{\partial w}{\partial x} \right) \tag{12}$$

with

$$q = \frac{\rho_a v^2}{2}, \qquad \beta = \sqrt{M_\infty^2 - 1}, \qquad \omega_{\mathrm{o}} = \left(\frac{D_{11}}{\rho h a^4} \right)^{\frac{1}{2}}$$

$$g_a = \frac{\rho_a v (M_\infty^2 - 2)}{\rho h \omega_{\mathrm{o}} \beta^3} \quad \text{and} \quad \lambda = \frac{2qa^3}{\beta D_{11}}$$

where P_a is the aerodynamic loading; v is the velocity of airflow; M_∞ is the Mach number; q is the dynamic pressure; ρ_a is the air mass density; g_a is nondimensional aerodynamic damping; λ is

nondimensional aerodynamic pressure; D_{11} is the first entry of the flexural stiffness matrix $D(1, 1)$, which depends on both T and n; and a is the panel length in the flow direction.

Governing Equations

By using the principle of virtual work and Eqs. (6), (7), (10), and (11), the governing equation of thermal postbuckling and nonlinear flutter of a functionally graded material plate can be derived as follows:

$$\delta W = \delta W_{\text{int}} - \delta W_{\text{ext}} = 0 \tag{13}$$

The internal virtual work δW_{int} is given as [33]

$$\begin{aligned}\delta W_{\text{int}} &= \int_A (\{\delta\varepsilon_m\}^T\{N\} + \{\delta\kappa\}^T\{M\} + \beta\{\delta\gamma\}^T\{R\})\,\mathrm{d}A \\ &= \{\delta w\}^T([K] - [K_T] + \tfrac{1}{2}[N1] + \tfrac{1}{3}[N2])\{w\} - \{\delta w\}^T(\{P_T\})\end{aligned} \tag{14}$$

where $\{w\} = [w \;\; \phi_x \;\; \phi_y \;\; u \;\; v]$ is the nodal-displacement vector; $[K]$ and $[K_T]$ are the linear stiffness matrix and the thermal geometric stiffness matrix; $[N1]$ and $[N2]$ are the first- and second-order nonlinear stiffness matrices, respectively; β is a shear correction factor; and $\{P_T\}$ is the thermal load vector.

On the other hand, the external virtual work δW_{ext} is given as [33]

$$\begin{aligned}\delta W_{\text{ext}} &= \int_A \begin{pmatrix} -I_o(\{\delta u\}^T\{\ddot{u}\} + \{\delta v\}^T\{\ddot{v}\} + \{\delta w\}^T\{\ddot{w}\}) \\ -I_2(\{\delta\phi_x\}^T\{\ddot{\phi}_x\} + \{\delta\phi_y\}^T\{\ddot{\phi}_y\}) + \{\delta w\}^T P_a \end{pmatrix}\mathrm{d}A \\ &= -\{\delta w\}^T[M]\{\ddot{w}\} - \{\delta w_b\}^T[G]\{\dot{w}_b\} - \{\delta w_b\}^T\lambda[A_a]\{w_b\}\end{aligned} \tag{15}$$

where

$$(I_o, I_2) = \int_{-h/2}^{h/2} \rho(z)(1, z^2)\,\mathrm{d}z$$

where h denotes the plate thickness, $[M]$ is the mass matrix, $[G]$ is the aerodynamic damping matrix, and $[A_a]$ is the aerodynamic influence matrix.

By substituting Eqs. (14) and (15) into Eq. (13), the governing equations for a functionally graded material plate under the combined action of aerodynamic and thermal loads can be obtained as

$$\begin{aligned}&\begin{bmatrix}[M_b] & 0 & 0 \\ 0 & [M_\phi] & 0 \\ 0 & 0 & [M_m]\end{bmatrix}\begin{Bmatrix}\{\ddot{W}_b\} \\ \{\ddot{W}_\phi\} \\ \{\ddot{W}_m\}\end{Bmatrix} + \begin{bmatrix}[G_b] & 0 & 0 \\ 0 & 0 & 0 \\ 0 & 0 & 0\end{bmatrix}\begin{Bmatrix}\{\dot{W}_b\} \\ \{\dot{W}_\phi\} \\ \{\dot{W}_m\}\end{Bmatrix} \\ &+ \left(\lambda\begin{bmatrix}[A_{ab}] & 0 & 0 \\ 0 & 0 & 0 \\ 0 & 0 & 0\end{bmatrix} + \begin{bmatrix}[K_b] & [K_{b\phi}] & 0 \\ [K_{\phi b}] & [K_\phi] & [K_{\phi m}] \\ 0 & [K_{m\phi}] & [K_m]\end{bmatrix} - \begin{bmatrix}[K_{Tb}] & 0 & 0 \\ 0 & 0 & 0 \\ 0 & 0 & 0\end{bmatrix}\right. \\ &\left. + \tfrac{1}{2}\begin{bmatrix}[N1_{nm} + N1_{n\phi}] & [N1_{b\phi}] & [N1_{bm}] \\ [N1_{\phi b}] & 0 & 0 \\ [N1_{mb}] & 0 & 0\end{bmatrix} + \tfrac{1}{3}\begin{bmatrix}[N2_b] & 0 & 0 \\ 0 & 0 & 0 \\ 0 & 0 & 0\end{bmatrix}\right) \\ &\times\begin{Bmatrix}\{W_b\} \\ \{W_\phi\} \\ \{W_m\}\end{Bmatrix} = \begin{Bmatrix}0 \\ \{P_{\phi T}\} \\ \{P_{mT}\}\end{Bmatrix}\end{aligned} \tag{16}$$

or, simply,

$$\begin{aligned}&[M]\{\ddot{W}\} + [G]\{\dot{W}\} + ([K] - [K_T] + \lambda[A_a] + \tfrac{1}{2}[N1] \\ &\quad + \tfrac{1}{3}[N2])\{W\} = \{P_T\}\end{aligned} \tag{17}$$

Solution Procedures

The solution of the governing equation (17) is assumed to be as follows:

$$\{W\} = \{W_s\} + \{W_t\} \tag{18}$$

where $\{W_s\}$ is the time-independent particular solution, which means the large thermal deflection, and $\{W_t\}$ is the time-dependent homogenous solution.

Substituting Eq. (18) into the governing equation (17),

$$\begin{aligned}&[M]\{\ddot{W}_t\} + [G]\{\dot{W}_t\} + ([K] - [K_T] + \lambda[A_a])(\{W_s\} + \{W_t\}) \\ &\quad + \tfrac{1}{2}([N1]_s + [N1]_t)(\{W_s\} + \{W_t\}) + \tfrac{1}{3}([N2]_s + [N2]_t \\ &\quad + 2[N2]_{st})(\{W_s\} + \{W_t\}) = \{P_T\}\end{aligned} \tag{19}$$

Equation (19) represents the general equation for the thermal buckling and nonlinear flutter of a functionally graded material plate under the combined effect of aerodynamic and thermal loads. The subscripts s and t indicate that the relevant matrix depends on the static or dynamic displacements, respectively.

Separating the static and dynamic terms of Eq. (19), the following two equations can be obtained :

$$([K] - [K_T] + \lambda[A_a] + \tfrac{1}{2}[N1]_s + \tfrac{1}{3}[N2]_s)\{W_s\} = \{P_T\} \tag{20}$$

$$\begin{aligned}&[M]\{\ddot{W}_t\} + [G]\{\dot{W}_t\} + ([K] - [K_T] + \lambda[A_a] + \tfrac{1}{2}[N1]_t \\ &\quad + \tfrac{1}{3}[N2]_t)\{W_t\} + ([N1]_s + [N2]_{st} + [N2]_s)\{W_t\} = 0\end{aligned} \tag{21}$$

Static Aerothermal Buckling

The solution procedure using the Newton–Raphson method for the aerothermal postbuckling analysis of a functionally graded material plate is presented as follows.

Introducing the function $\{\Psi(\mathrm{W})\}$ to Eq. (20),

$$\begin{aligned}\{\Psi(W_s)\} &= ([K] - [K_T] + \lambda[A_a] + \tfrac{1}{2}[N1]_s \\ &\quad + \tfrac{1}{3}[N2]_s)\{W_s\} - \{P_T\} = 0\end{aligned} \tag{22}$$

Equation (22) can be written in the form of a truncated Taylor series expansion as

$$\{\Psi(W_s + \delta W)\} = \{\Psi(W_s)\} + \frac{\mathrm{d}\{\Psi(W_s)\}}{\mathrm{d}(W_s)}\{\delta W\} \cong 0 \tag{23}$$

where

$$\frac{\mathrm{d}\{\Psi(W_s)\}}{\mathrm{d}(W_s)} = ([K] - [K_T] + \lambda[A_a] + [N1]_s + [N2]_s) = [K_{\tan}] \tag{24}$$

Thus, the Newton–Raphson iteration procedure for the determination of the postbuckling deflection can be expressed as follows:

$$\{\Psi(W_s)\}_i = \left([K] - [K_T] + \lambda[A_a] + \tfrac{1}{2}([N1]_s)_i + \tfrac{1}{3}([N2]_s)_i\right)\{W_s\} - \{P_T\}$$

$$[K_{\tan}]_i\{\delta W\}_{i+1} = -\{\Psi(W_s)\}_i \;\; \{\delta W\}_{i+1} = -[K_{\tan}]^{-1}\{\Psi(W_s)\}_i$$

$$\{W_s\}_{i+1} = \{W_s\}_i + \{\delta W\}_{i+1}$$

Convergence occurs in the preceding procedure when the maximum value of $\{\delta W\}_{i+1}$ becomes less than a given tolerance ε_{tol} (i.e., $\max|\{W\}_{i+1}| \varepsilon_{\text{tol}}$).

Free Vibration

From Eq. (21), the equation of free vibration about a statically stable position could be stated as

$$[M]\{\ddot{W}_t\} + ([K] - [K_T] + \lambda[A_a] + [N1]_s + [N2]_s)\{W_t\} = 0 \tag{25}$$

This could be written as

$$[M]\{\ddot{W}_t\} + [K_{\tan}]\{W_t\} = 0 \tag{26}$$

Assuming the solution of the preceding differential equation to take the following form,

$$\{W_t\} = \bar{c}\{\Phi\}e^{\Omega t} \tag{27}$$

the generalized eigenvalue problem could be stated as

$$(\Omega^2[M] + [K_{\tan}])\{\Phi\} = 0 \tag{28}$$

Thus, the solution procedure would be, first, the solution of the static thermal deflection and the associated stiffness matrices by following the procedure outlined in the preceding section, and then, solving the eigenvalue problem of Eq. (28) for the free vibration of a thermally buckled functionally graded material plate.

Panel Flutter Under Thermal Effect

In this section, the procedure of determining the critical nondimensional dynamic pressure under the presence of thermal loading is presented. Equation (21) can be reduced for the solution of the linear (prebuckling and preflutter) problem to the following equation:

$$[M]\{\ddot{W}_t\} + [G]\{\dot{W}_t\} + ([K] - [K_T] + \lambda[A_a] + [N1]_s)\{W_t\} = 0 \tag{29}$$

applying new notation for the bending degree of freedom by combining the shear and bending degrees of freedom as

$$\{W_B\} = \begin{Bmatrix} W_b \\ W_\phi \end{Bmatrix} \tag{30}$$

Neglecting the in-plane and shear inertia terms will not bring significant error, because their natural frequencies are usually two to three orders of magnitude higher than the bending frequencies[30]. Separating Eq. (29) into membrane and transverse directions results in the following transverse dynamic equation:

$$[M_B]\{\ddot{W}_B\}_t + [G]\{\dot{W}_B\}_t + ([K_B] - [K_{TB}] + \lambda[A_{aB}] + [N1_{nmB}]_s - [K_{Bm}][K_m]^{-1}[K_{mB}])\{W_B\}_t = 0 \tag{31}$$

Note that the terms related to $[N2]$, $[N1_{n\phi}]$ and $[N1_{mB}]$ are dropped because they depend on $\{W_B\}$, which is essentially zero before buckling or flutter, whereas $[N1_{nmB}]_s$ term are kept because they depend on $\{W_m\}$, which might have nonzero values, depending on the in-plane boundary conditions.

Now assume the deflection function of the transverse displacement $\{W_B\}_t$ to be in the form of

$$\{W_B\}_t = \bar{c}\{\Phi_B\}e^{\Omega t} \tag{32}$$

where $\Omega = \alpha + i\omega$ is the complex panel motion parameter (α is the damping ratio and ω is the frequency), $\bar{c}$ is the amplitude of vibration, and $\{\Phi_B\}$ is the mode shape.

Substituting Eq. (32) into Eq. (31), the generalized eigenvalue problem can be obtained as

$$\bar{c}[-\kappa(M_B) + (\bar{K}_B)]\{\Phi_B\}e^{\Omega t} = \{0\} \tag{33}$$

where $[G_B] = \omega_o g_a[M_B]$, and κ is the nondimensional eigenvalue given by

$$\kappa = -\Omega^2 - \omega_o g_a \Omega \tag{34}$$

and

$$[\bar{K}_B] = [K_B] - [K_{TB}] + \lambda[A_{aB}] + [N1_{nmB}]_s - [K_{Bm}][K_m]^{-1}[K_{mB}] \tag{35}$$

From Eq. (33), we can write the generalized eigenvalue problem:

$$[-\kappa(M_B) + (\bar{K}_B)]\{\Phi_B\} = \{0\} \tag{36}$$

where κ is the eigenvalue and Φ_B is the mode shape, with the characteristic equation written as

$$|-\kappa[M_B] + [\bar{K}_B]| = \{0\} \tag{37}$$

Given that the values of κ are real for all values of λ below the critical value, an iterative solution can be used to determine the critical nondimensional dynamic pressure λ_{cr}.

Limit-Cycle Amplitude

In this section, the harmonic limit-cycle amplitude will be determined for a fluttering functionally graded material plate at temperatures less than the buckling temperature ($\{W_B\}_s = 0$). Following the same procedure outlined in the previous section, with the only difference being that nonlinear stiffness terms that depend on the transverse dynamic displacement ($\{W_B\}_t$) will be included to end up with the following equation:

$$\begin{bmatrix} M_B & 0 \\ 0 & 0 \end{bmatrix}\begin{Bmatrix} \ddot{W}_B \\ \ddot{W}_m \end{Bmatrix}_t + \begin{bmatrix} G_B & 0 \\ 0 & 0 \end{bmatrix}\begin{Bmatrix} \dot{W}_B \\ \dot{W}_m \end{Bmatrix}_t + \left(\begin{bmatrix} K_B & K_{Bm} \\ K_{mB} & K_m \end{bmatrix} - \begin{bmatrix} K_{TB} & 0 \\ 0 & 0 \end{bmatrix} + \lambda\begin{bmatrix} A_{aB} & 0 \\ 0 & 0 \end{bmatrix} + \begin{bmatrix} N1_{nmB} & 0 \\ 0 & 0 \end{bmatrix}_s\right)\begin{Bmatrix} W_B \\ W_m \end{Bmatrix}_t + \left(\frac{1}{2}\begin{bmatrix} N1_B & N1_{Bm} \\ N1_{mB} & 0 \end{bmatrix}_t + \frac{1}{3}\begin{bmatrix} N2_B & 0 \\ 0 & 0 \end{bmatrix}_t\right)\begin{Bmatrix} W_B \\ W_m \end{Bmatrix}_t = 0 \tag{38}$$

Separating the membrane displacement equation and the transverse displacement equation from Eq. (38),

$$[M_B]\{\ddot{W}_B\}_t + [G]\{\dot{W}_B\}_t + ([K_B] - [K_{TB}] + \lambda[A_{aB}] + [N1_{nmB}]_s)\{W_B\}_t + (\tfrac{1}{2}[N1_B]_t + \tfrac{1}{3}[N2_B]_t)\{W_B\}_t + ([K_{Bm}] + \tfrac{1}{2}[N1_{Bm}]_t)\{W_m\}_t = 0 \tag{39}$$

$$[K_{mB}]\{W_B\}_t + [K_m]\{W_m\}_t + \tfrac{1}{2}[N1_{mB}]_t\{W_B\}_t = 0 \tag{40}$$

Therefore, the in-plane displacement vector $\{W_m\}_t$ can be expressed in terms of the bending displacement vector $\{W_B\}_t$ as

$$\{W_m\}_t = -([K_m]^{-1}[K_{mB}] + \tfrac{1}{2}[K_m]^{-1}[N1_{mB}]_t)\{W_B\}_t \tag{41}$$

Substituting Eq. (41) into Eq. (39),

$$[M_B]\{\ddot{W}_B\}_t + [G_B]\{\dot{W}_B\}_t + ([K_B] - [K_{TB}] + \lambda[A_{aB}] + [N1_{nmB}]_s - [K_{Bm}][K_m]^{-1}[K_{mB}])\{W_B\}_t + (\tfrac{1}{2}[N1_B]_t - \tfrac{1}{2}[K_{Bm}][K_m]^{-1}[N1_{mB}]_t - \tfrac{1}{2}[N1_{Bm}]_t[K_m]^{-1}[K_{mB}])\{W_B\}_t + (\tfrac{1}{3}[N2_B]_t - \tfrac{1}{4}[N1_{Bm}]_t[K_m]^{-1}[N1_{mB}]_t)\{W_B\}_t = 0 \tag{42}$$

A procedure similar to those described earlier can be used to write the equation of motion in the form

$$\bar{c}[-\kappa(M_B) + (\bar{K}_B)]\{\Phi_B\}e^{\Omega t} = \{0\} \tag{43}$$

where

$$[\bar{K}_B] = [K_B] - [K_{TB}] + \lambda[A_{aB}] + [N1_{nmB}]_s - [K_{Bm}][K_m]^{-1}[K_{mB}] + \tfrac{1}{2}[N1_B]_t - \tfrac{1}{2}[K_{Bm}][K_m]^{-1}[N1_{mB}]_t - \tfrac{1}{2}[N1_{Bm}]_t[K_m]^{-1}[K_{mB}] + \tfrac{1}{3}[N2_B]_t - \tfrac{1}{4}[N1_{Bm}]_t[K_m]^{-1}[N1_{mB}]_t \tag{44}$$

Because the nonlinear stiffness terms of the preceding equation depend on the amplitude of the vibration, an iterative scheme should

Table 1 Temperature-dependence coefficients for silicon nitride and nickel [29]

Properties	Material	P_{-1}	P_0	P_1	P_2	P_3
E, MPa	Si_3N_4	0	348.43e9	−3.07e − 4	2.2e − 7	−8.9e − 11
	Nickel	0	223.95e9	−2.79e − 4	3.9e − 9	0
ν	Si_3N_4	0	0.24	0	0	0
	Nickel	0	0.31	0	0	0
α	Si_3N_4	0	5.8723e − 6	9.09e − 4	0	0
	Nickel	0	9.9209e − 6	8.71e − 4	0	0
ρ, kg/m^3	Si_3N_4			2370		
	Nickel			8900		

be used. The following algorithm outlines the steps used in the iterative procedure [34]:

1) Normalize the eigenvector $\{\Phi_B\}$ obtained at the flutter point using the maximum displacement.
2) Select a value for the amplitude $\bar{c}$.
3) Evaluate the linear and nonlinear stiffness terms.
4) Change the value of the nondimensional aerodynamic pressure λ.
5) Solve the eigenvalue problem for κ.
6) If coalescence occurs, proceed, else go to step 4.
7) Check the differences between the obtained eigenvector and the initial one, if small, proceed, else normalize the eigenvector as described in step 1 and go to step 3.
8) The obtained dynamic pressure corresponds to the initially given amplitude.
9) Go to step 2.

It should be noted that the aforementioned procedure is valid only for the case when panel flutter occurs but the plate is not buckled or when the dynamic pressure is high enough that the buckled plate becomes flat again, which does not cover the region of chaotic vibration.

Numerical Results and Discussions

In this section, the effect of the volume fraction exponent n and different boundary conditions on the static and dynamic response will be demonstrated. Numerical analyses for the thermal postbuckling and nonlinear flutter of a functionally graded material with temperature-dependent material properties are performed using the nonlinear finite element. A uniform 6×6 finite element mesh of nine-node elements are employed. The reduced-order technique is used for integrating terms related to the transverse shear to avoid shear locking.

Aerothermal Buckling Analysis

Thermal buckling and postbuckling analysis with and without aerodynamic loading and with uniform temperature increase are carried out for an FGM panel that is a mixture of nickel and silicon nitride (Si_3N_4) to figure out the effect of the volume fraction exponent n, the dynamic pressure, and the different boundary conditions on the buckling characteristics of the FGM panel. The geometry of the plate is chosen to be $0.38 \times 0.305 \times 0.002$ m. The plate edge supports are immovable in the in-plane direction. The material properties are assumed to be temperature-dependent according to the following relation [29]:

$$P = P_o(P_{-1}T^{-1} + 1 + P_1T + P_2T^2 + P_3T^3) \tag{45}$$

The coefficients P_o, P_{-1}, P_1, P_2, and P_3 for Young's modulus E; the Poisson ratio ν; and the thermal expansion coefficient α of nickel and silicon nitride are given in Table 1. Uniform temperature change was applied to the plate.

Figure 2 illustrates the effect of the volume fraction exponent on the buckling characteristics of a clamped FGM panel. It is seen in the figure that decreasing the volume fraction exponent results in a higher buckling temperature and lower postbuckling deflection, because the Si_3N_4 volume fraction increases with decreasing the volume fraction exponent, which in turn leads to lower thermal expansion coefficient and higher modulus of elasticity than that of the nickel. It is also seen that the responses that correspond to properties intermediate to those of the metal and the ceramic lie between those of the metal and ceramic, which is consistent with what is mentioned by Reddy [20].

As seen in Fig. 3 for functionally graded material panels with simply supported edges, there is no buckling phenomenon, because any small temperature rise results in a prompt transverse deflection of the panel, due to structural asymmetry about the middle plane of the FGM panel that makes all simply supported FGM panels lose their buckling phenomena.

Figure 4 illustrates the effect of changing the value of the dynamic pressure on the buckling temperature and postbuckling deflection of the nickel/silicon-nitride FGM clamped panel with the volume fraction exponent n equals one ($n = 1$). D_{11} is evaluated at T_{ref} and $n = 1$. It is seen clearly that the presence of the airflow increases the stiffness of the panel through the aerodynamic stiffness matrix,

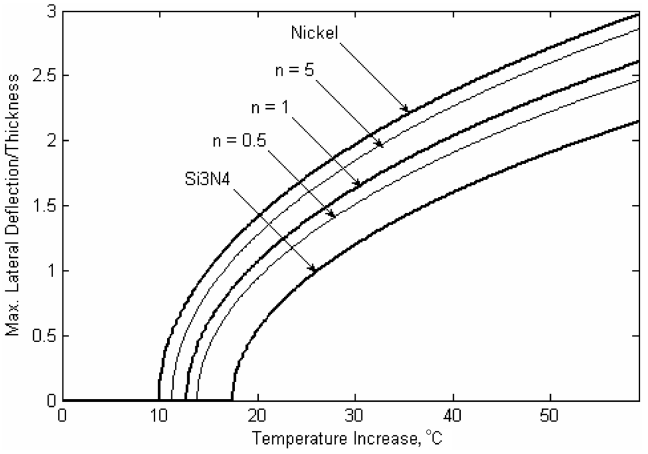

Fig. 2 Postbuckling deflection for a clamped FGM panel with different volume fraction exponents n.

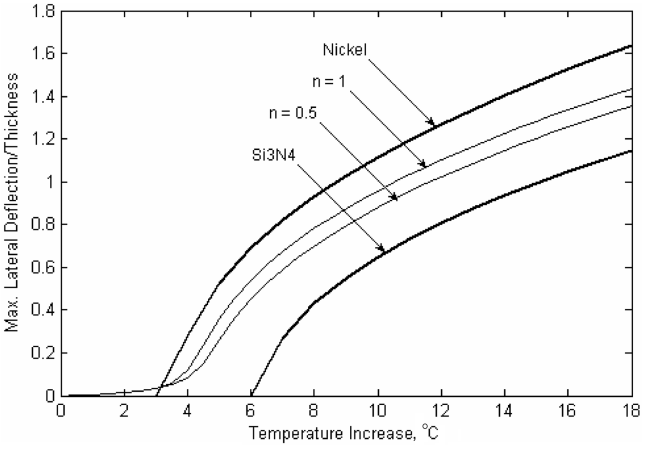

Fig. 3 Postbuckling deflection for a simply supported FGM panel with different volume fraction exponents n.

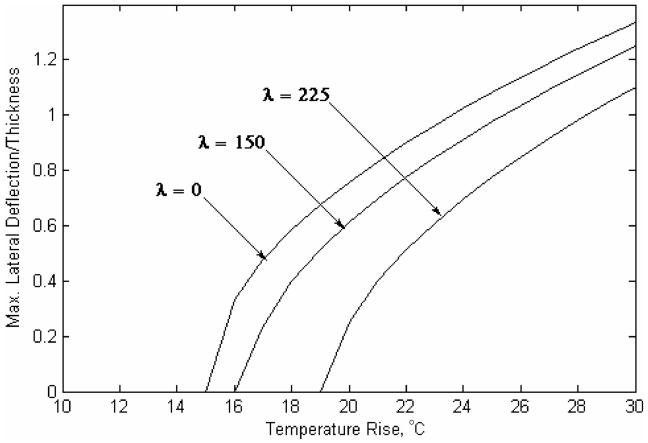

Fig. 4 Effect of the different values of the dynamic pressure on the buckling characteristics of a clamped FGM panel with $n = 1$.

which results in a higher buckling temperature and a lower postbuckling deflection; that is, it is conservative to neglect the presence of the air when performing thermal buckling analysis.

Although the ceramic panel response seems to be superior to that of the FGM panel, using the ceramic panel results in a structural integrity problem, due to the brittleness of the ceramic. So it is worthwhile noting that increasing the ceramic volume fraction is bounded by structural integrity aspects.

Free Vibration

The vibration characteristics of a nickel/silicon-nitride FGM clamped panel with different volume fraction exponents n are studied. The material properties, temperature distribution, and dimensions of the plate are the same as those used in the previous section.

Figure 5 illustrates the effect of temperature increase and the volume fraction exponent on the fundamental frequency. It is seen in the figure that for all values of n, the frequency decreases with temperature, due the decreasing stiffness in the prebuckling region, whereas after buckling, the frequency increases with temperature as the plate stiffness increases, due to the addition of the nonlinear terms. It is also seen that increasing the ceramic volume fraction through decreasing the volume fraction exponent results in a higher fundamental frequency in both of the prebuckling and postbuckling regions, and this is due to the lower mass density of the ceramic than that of the metal. It is seen in the previous section that the ceramic has lower postbuckling deflection compared with that of the metal, which in turn results in a lower stiffness in the postbuckling region (i.e., lower fundamental frequency). But this is not the case according to Fig. 5, because the mass density of the ceramic is almost one-third that of the metal, which suppresses the effect of the lower postbuckling deflection of the ceramic.

It should be noted that the ceramic natural frequencies may not be favorable regarding the response of the FGM panel to acoustic loading, due to its higher fundamental frequencies. So it is going to be a matter of a tradeoff between the thermal response and the acoustic response.

Predicting Panel Flutter Boundaries

In this section, the stability boundaries of an FGM panel with clamped edges and with different volume fraction exponents n will be studied. The results of the combined loading stability boundaries were obtained by two different methods. To obtain the flutter boundary, the dynamic pressure is increased at a certain temperature until the coalescence of two eigenmodes (i.e., until flutter occurs). To have the thermal buckling boundary, the critical buckling temperature is calculated with dynamic pressure as a parameter.

An FGM panel under the effect of thermal and aerodynamic loading is presented in Fig. 6 in terms of the critical temperature boundary and linear flutter boundary. D_{11} is evaluated at T_{ref} and $n = \infty$ (i.e., D_{11} is evaluated using the nickel properties at room temperature). The area of the graph is divided into three regions: the flat-panel region, in which the panel is stable (i.e., neither buckling nor panel flutter occurred); the buckled region, in which the thermal stresses overcome the panel stiffness and aerodynamic stiffness, and the panel undergoes static instability under in-plane thermal loading; and the third region is the flutter region, in which the panel undergoes dynamic instability under the influence of aerodynamic pressure. Thus, the wider the flat-panel region, the more stable the panel. It is also seen in Fig. 6 that decreasing the volume fraction exponent n results in a wider flat-panel region and, in turn, a more stable panel.

Limit-Cycle Amplitude

In this section, the limit-cycle amplitude will be determined for a fluttering functionally graded material plate at temperatures less than the buckling temperature ($\{W_b\}_s = 0$), illustrating the effect of the volume fraction exponent on the nonlinear FGM panel flutter.

Figure 7 presents the variation of the limit-cycle amplitude of a clamped FGM panel with the variation of both the nondimensional dynamic pressure and the volume fraction exponent at a 6°C temperature increase. D_{11} is evaluated at T_{ref} and $n = \infty$. It is seen in the figure that the limit-cycle amplitude increases with increasing both the volume fraction exponent and the dynamic pressure. Also, it is seen that the response of the FGM plate is intermediate to both of the ceramic and the metal.

Figure 8 presents a full map of the variation of both the limit-cycle amplitude and the postbuckling deflection with the dynamic pressure for different values of the temperature increase, illustrating the distinction between the static and dynamic regions. The volume

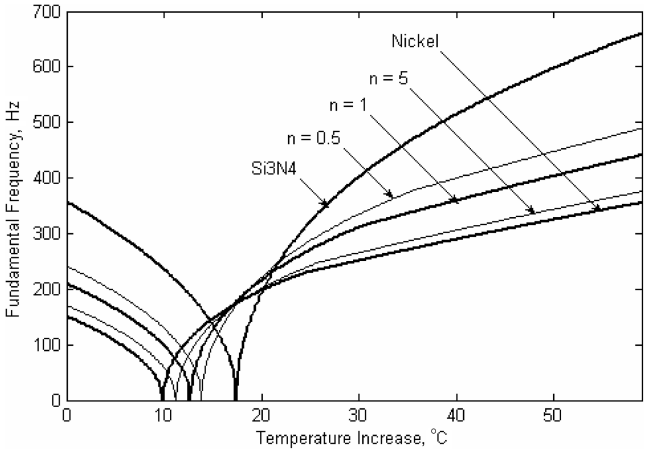

Fig. 5 Natural frequencies in the prebuckled and postbuckled regions for different volume fraction exponents n.

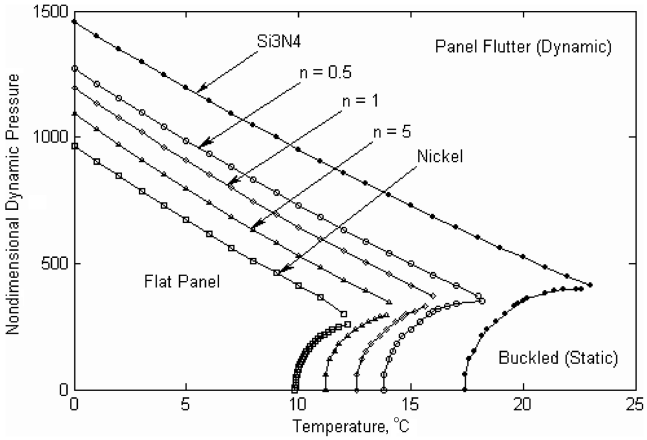

Fig. 6 The effectiveness of the volume fraction exponent n on the stability boundaries of an FGM clamped panel.

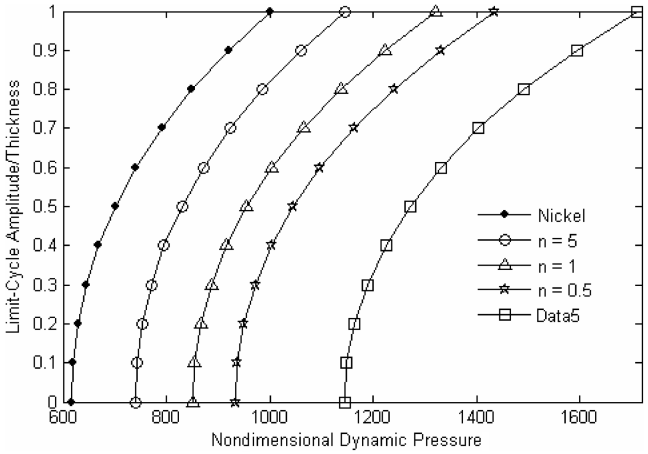

Fig. 7 Variation of the limit-cycle amplitude with dynamic pressure at a temperature increase of 6°C for a clamped FGM panel.

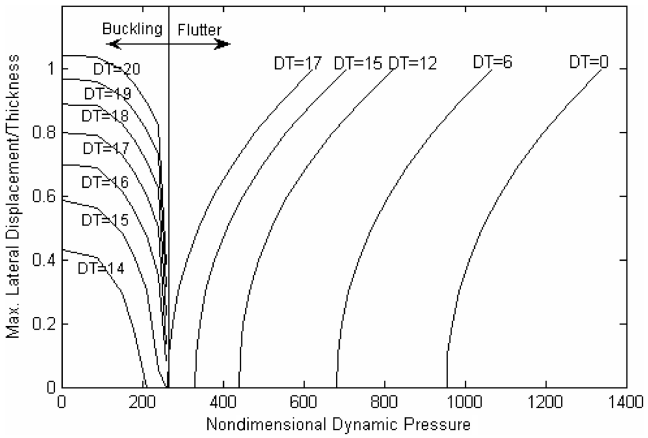

Fig. 8 Full map of the variation of the limit-cycle amplitude and the postbuckling deflection with the dynamic pressure for $n = 1$.

fraction exponent in this figure was chosen to equal one ($n = 1$), and D_{11} is evaluated at T_{ref} and $n = 1$.

Conclusions

An efficient finite element formulation was presented for the analysis of supersonic nonlinear panel flutter and thermal buckling characteristics of an FGM panel made of nickel and silicon nitride. Shear deformable plate theory based on temperature-dependent material properties and von Kármán moderately large deflection was considered in the formulation. The material properties were assumed to vary the through-the-thickness direction based on a simple power law distribution. The aerodynamic forces were modeled using the quasi-steady first-order piston theory. An approach based on thermal strain being a cumulative physical quantity was adopted to take into account the temperature dependency of material properties.

The effectiveness of the volume fraction exponent and the boundary conditions on thermal buckling, fundamental frequency, and nonlinear panel flutter characteristics of the FGM panel was studied. The results showed that the presence of the silicon nitride with the nickel enhances the buckling characteristics of the panel through increasing the buckling temperature and decreasing the postbuckling deflection. Functionally graded material panels with simply supported edges were found to have no distinguished buckling phenomena, because any small temperature rise results in a prompt transverse deflection of the panel, due to structural asymmetry about the middle plane. For a given temperature, it was also found that decreasing the volume fraction exponent enhances flutter characteristics through increasing the critical dynamic pressure. The presence of aerodynamic flow results in higher buckling temperature and lower postbuckling deflection (i.e., results in a stiffer panel). It is found that the limit-cycle amplitude increases with increasing both the volume fraction exponent and the dynamic pressure.

References

[1] Tauchart, T. R., "Thermally Induced Flexure, Buckling, and Vibration of Plates," *Applied Mechanics Reviews*, Vol. 44, No. 8, Aug. 1991, pp. 347–360.

[2] Thornton, E. A., "Thermal Buckling of Plates and Shells," *Applied Mechanics Reviews*, Vol. 46, No. 10, Oct. 1993, pp. 485–506.

[3] Gray, C. C., and Mei, C., "Finite Element Analysis of Thermal Postbuckling and Vibrations of Thermally Buckled Composite Plates," *32nd AIAA/ASME/ASCE/AHS/ASC Structures, Structural Dynamics, and Materials Conference*, Pt. 4, A91-31826 12-39, AIAA, Washington, DC, 1991, pp. 2996–3007.

[4] Shi, Y., Lee, R. Y. Y., and Mei, C., "Thermal Postbuckling of Composite Plates Using the Finite Element Modal Coordinate Method," *Journal of Thermal Stresses*, Vol. 22, No. 6, Aug. 1999, pp. 595–614.

[5] Jones, R., and Mazumdar, J., "Vibration and Buckling of Plates at Elevated Temperatures," *International Journal of Solids and Structures*, Vol. 16, No. 1, 1980, pp. 61–70.

[6] Shi, Y., Lee, R. Y., and Mei, C., "Coexiting Thermal Postbuckling of Composite Plates with Initial Imperfections Using Finite Element Modal Method," *Journal of Thermal Stresses*, Vol. 22, No. 6, 1999, pp. 595–614.

[7] Jordan, P. F., "The Physical Nature of Panel Flutter," *Aero Digest*, Vol. 72, No. 2, Feb. 1956, pp. 34–38.

[8] Mei, C., Abdel-Motagaly, K., and Chen, R., "Review of Nonlinear Panel Flutter at Supersonic and Hypersonic Speeds," *Applied Mechanics Reviews*, Vol. 52, No. 10, 1999, pp. 321–332.

[9] Liaw, D. G., "Nonlinear Supersonic Flutter of Laminated Composite Plates Under Thermal Loads," *Computers and Structures*, Vol. 65, No. 5, 1997, pp. 733–740.

[10] Abdel-Motagaly, K., Chen, R., and Mei, C., "Effects of Flow Angularity on Nonlinear Supersonic Flutter of Composite Panels Using Finite Element Method," *40th AIAA/ASME/ASCE/AHS/ASC Structures, Structural Dynamics, and Materials Conference*, AIAA, Reston, VA, 1999, pp. 1963–1972.

[11] Mei, C., "A Finite-Element Approach for Nonlinear Panel Flutter," *AIAA Journal*, Vol. 15, No. 8, 1977, pp. 1107–1110.

[12] Dixon, I. R., and Mei, C., "Finite Element Analysis of Large-Amplitude Panel Flutter of Thin Laminates," *AIAA Journal*, Vol. 31, No. 4, 1993, pp. 701–707.

[13] Xue, D. Y., and Mei, C., "Finite Element Nonlinear Panel Flutter with Arbitrary Temperatures in Supersonic Flow," *AIAA Journal*, Vol. 31, No. 1, 1993, pp. 154–162.

[14] Sarma, B. S., and Varadan, T. K., "Nonlinear Panel Flutter by Finite Element Method," *AIAA Journal*, Vol. 26, No. 5, 1987, pp. 566–574.

[15] Dongi, F., Dinkler, D., and Kroplin, B., "Active Panel Flutter Suppression Using Self-Sensing Piezoactuators," *AIAA Journal*, Vol. 34, No. 6, 1996, pp. 1224–1230.

[16] Lee, I., Roh, J.-H., and Oh, I.-K., "Aerothermoelastic Phenomena of Aerospace and Composite Structures," *Journal of Thermal Stresses*, Vol. 26, No. 6, 2002, pp. 525–546.

[17] Dai, K. Y., Liu, G. R., Han, X., and Lim, K. M., "Thermomechanical Analysis of Functionally Graded Material (FGM) Plates Using Element-Free Galerkin Method," *Computers and Structures*, Vol. 83, Nos. 17–18, 2005, pp. 1487–1502.

[18] Birman, V., "Stability of Functionally Graded Shape Memory Alloy Sandwich Panels," *Smart Materials and Structures*, Vol. 6, No. 3, 1997, pp. 278–286.

[19] El-Abbasi, N., and Meguid, S. A., "Finite Element Modeling of the Thermoelastic Behavior of Functionally Graded Plates and Shells," *International Journal of Computational Engineering Science*, Vol. 1, No. 1, 2000, pp. 151–165.

[20] Reddy, J. N., "Analysis of Functionally Graded Plates," *International Journal for Numerical Methods in Engineering*, Vol. 47, Nos. 1–3, 2000, pp. 663–684.

[21] He, X. Q., Ng, T. Y., Sivashanker, S., and Liew, K. M., "Active Control of FGM Plates with Integrated Piezoelectric Sensors and Actuators," *International Journal of Solids and Structures*, Vol. 38, No. 9, 2001, pp. 1641–1655.

[22] Javaheri, R., and Eslami, M. R., "Thermal Buckling of Functionally Graded Plates Based on Higher Order Theory," *Journal of Thermal Stresses*, Vol. 25, No. 7, 2002, pp. 603–625.

[23] Woo, J., Meguid, S. A., and Liew, K. M., "Thermomechanical Postbuckling Analysis of Functionally Graded Plates and Shallow Cylindrical Shells," *Acta Mechanica*, Vol. 165, Nos. 1–2, 2003, pp. 99–115.

[24] Yang, J., Kitipornchai, S., and Liew, K. M., "Non-Linear Analysis of the Thermo-Electro-Mechanical Behavior of Shear Deformable FGM Plates with Piezoelectric Actuators," *International Journal for Numerical Methods in Engineering*, Vol. 59, No. 12, 2004, pp. 1605–1632.

[25] Zenkour, A. M., "Generalized Shear Deformation Theory for Bending Analysis of Functionally Graded Plates," *Journal of Applied Mathematical Modeling*, Vol. 30, No. 1, 2005, pp. 67–84.

[26] Kim, Y. W., "Temperature Dependent Vibration Analysis of Functionally Graded Rectangular Plates," *Journal of Sound and Vibration*, Vol. 284, Nos. 3–5, 2005, pp. 531–549.

[27] Batra, R. C., and Jin, J., "Natural Frequencies of a Functionally Graded Anisotropic Rectangular Plate," *Journal of Sound and Vibration*, Vol. 282, Nos. 1–2, 2005, pp. 509–516.

[28] Qian, L. F., and Batra, R. C., "Design of Bidirectional Functionally Graded Plate for Optimal Natural Frequencies," *Journal of Sound and Vibration*, Vol. 280, Nos. 1–2, 2005, pp. 415–424.

[29] Parakash, T., and Ganapathi, M., "Supersonic Flutter Characteristics of Functionally Graded Flat Panels Including Thermal Effects," *Composite Structures*, Vol. 72, No. 1, 2006, pp. 10–18.

[30] Guo, X., "Shape Memory Alloy Applications on Control of Thermal Buckling, Panel Flutter and Random Vibration of Composite Panels," Ph.D. Dissertation, Mechanical Engineering Dept., Old Dominion Univ., Norfolk, VA, 2005.

[31] Tawfik, M., Ro, J. J., and Mei, C., "Thermal Postbuckling and Aeroelastic Behavior of Shape Memory Alloy Reinforced Plates," *Smart Materials and Structures*, Vol. 11, No. 2, 2002, pp. 297–307.

[32] Guo, X., "Shape Memory Alloy Applications on Control of Thermal Buckling, Panel Flutter and Random Vibration of Composite Panels," Ph.D. Dissertation, Mechanical Engineering Dept., Old Dominion Univ., Norfolk, VA, 2005.

[33] Park, J. S., Kim, J. H., and Moon, S. H., "Vibration of Thermally Post-Buckled Composite Plates Embedded with Shape Memory Alloy Fibers," *Composite Structures*, Vol. 63, No. 2, 2004, pp. 179–188.

[34] Xue, D. Y., "Finite Element Frequency Domain Solution of Nonlinear Panel Flutter with Temperature Effects and Fatigue Life Analysis," Ph.D. Dissertation, Mechanical Engineering Dept., Old Dominion Univ., Norfolk, VA, 1991.